

OLYMPUS Status Report

OLYMPUS Collaboration

1 Introduction

2 This is intended to be a brief report on developments regarding the OLYMPUS
3 experiment since the last PRC meeting.

4 At the last PRC meeting we reported on several topics:

- 5 - the analysis of the detector position survey ($< 100 \mu\text{m}$),
- 6 - fitting the magnetic field measurements ($< 19 \text{ G}$),
- 7 - the beam energy calibration (0.01%),
- 8 - studies to understand and optimize the Møller/Bhabha calorimeter and the 12°
9 GEM and MWPC telescopes,
- 10 - the calibration of the time of flight detectors,
- 11 - the first tracking results using the elastic arm algorithm with a preliminary
12 yield distribution, and
- 13 - the status of our Monte Carlo generator including radiative corrections.

14 During the closed session we outlined our immediate plans:

- 15 - additional manpower to work on the luminosity detectors,
- 16 - separate fit to the magnetic field in the region of the symmetric Møller/Bhabha
17 event trajectories,
- 18 - beam position monitor calibration,
- 19 - improve detector calibrations using tracking, and

20 - Monte Carlo simulation with radiative corrections.

21 The recommendations from the PRC added:

22 - completing the digitization of all detectors in the Monte Carlo,

23 - increasing manpower and expertise on software and analysis, and

24 - developing an alternative, traditional approach to tracking reconstruction,

25 The PRC report also requested that this report address the luminosity determination
26 and characterize the tracking performance.

27 In the following we will try to address all of the above. The work is not finished and
28 there have been set-backs but steady progress is being made. For brevity point-form
29 will be used as much as possible. Detailed descriptions or explanations, if needed, are
30 perhaps more easily communicated via phone or video conference if necessary.

31 **2 Manpower**

32 The principal people working on the OLYMPUS analysis are outlined in the following.
33 The area(s) in which they are most active is also given. Certainly this list is not
34 complete and many names have been omitted for simplicity.

35 - D. Khanefit (Mainz) is taking a more active role on the SYMB. He came to
36 MIT from mid-November to mid-December to gain experience with the analysis
37 framework and is now working on the digitization of the SYMB. Dmitry joins
38 R. Perez Benito (Mainz) who is also working on the SYMB (see below).

39 - C. O'Connor (MIT) is now also working on the SYMB analysis (see below).

40 - U. Schneekloth (DESY) has been working on the BPM survey, calibration, and
41 analysis (see below) needed for the SYMB analysis.

42 - B. Henderson (MIT) is now working on the analysis of 12° detector tele-
43 scopes (see below). Unfortunately Ö. Ates (Hampton) will be leaving shortly.
44 D. Veretennikov (PNPI) continues working on the 12° detectors.

45 - Y. Naryshkin (PNPI) is comparing the luminosity determined from the SYMB
46 with the results from the 12° detectors.

47 - L.D. Ice (ASU), R. Russell (MIT), and N. Akopov (AANL) together with
48 other members of the AANL group continue to care for the TOF calibration,

49 simulation, and analysis now using the reconstructed tracking information (see
50 below).

51 - R. Russell and A. Schmidt (MIT) have finished the Monte Carlo generator
52 incorporating radiative corrections (see below).

53 - J. Bernauer (MIT) continues work on track reconstruction. Recently he ex-
54 tending the tracks to the TOF detectors (see below) and is now working to add
55 the BPM data into the analysis and Monte Carlo framework. He also serves
56 as software coordinator and directs most of the analysis efforts.

57 - D. Hasell (MIT) is pursuing an alternative approach to track reconstruction
58 (see below).

59 - M. Kohl (Hampton) continues as luminosity and physics coordinator. Unfor-
60 tunately J. Diefenbach (now at Mainz) who contributed so much has less time
61 to help with OLYMPUS.

62 - N. D'Ascenzo (DESY) and N. Akopov are working on analyzing the recon-
63 structed track data (see below).

64 - K. Suvorov (PNPI) is studying pion electroproduction using the Monte Carlo
65 pion generator implemented by L.D. Ice.

66 **3 Luminosity**

67 The OLYMPUS luminosity monitors include the symmetric Møller/Bhabha detector
68 and the 12° telescopes of GEM and MWPC detectors.

69 **3.1 Symmetric Moller / Bhabha Calorimeter**

70 The symmetric Møller/Bhabha detector, SYMB, should provide the best statistics
71 for our measurement of the luminosity. There are two parts to this: getting a stable,
72 reliable measure of the number of symmetric scattering events, and, in support of
73 this, accurately simulating the processes with the Monte Carlo.

74 - R. Perez Benito has been working on a differential non-linearity (DNL) algo-
75 rithm to smooth the data produced by the SYMB electronics so the coincidence
76 peak can be more accurately found, fit, and integrated. This is illustrated in

Fig. 1. With DNL corrections, the ratio found between electron and positron

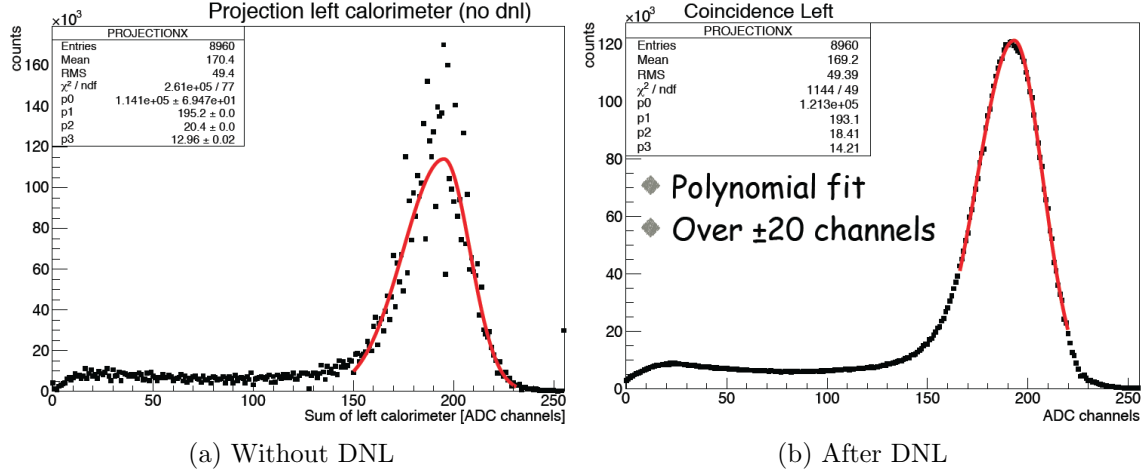


Figure 1: Effect of differential non-linearity correction to SYMB histograms.

77

runs is 1.640 ± 0.006 .

78

79

- R. Perez Benito has also measured that the SYMB pedestals are stable over time and do not contribute any noticeable effect.

80

81

- As mentioned D. Khanefit is working on simulating the SYMB in the Monte Carlo. His focus is on digitizing the simulated signal to match the real detector's electronics and modeling the detector's physical response and light propagation.

82

83

84

- C. O'Connor has been investigating the SYMB also with Monte Carlo. One of the questions was about the "legs" to the left and below the coincidence peak observed in the data (see Fig. 2). These are qualitatively reproduced in the Monte Carlo and found to arise from events near the edge of the collimator on one side of the beamline with the corresponding, symmetrically scattered particle striking the edge of the other collimator on the opposite side. This other particle showers or multiple scatters through some portion of the collimator, resulting in energy loss producing the "legs".

85

86

87

88

89

90

91

92

- The previous plots showed the SYMB coincidence histogram with a logarithmic scale. Plotted with a linear scale, Fig. 3, the coincidence peak is clearly separated from an almost flat background. Integrating over a square area centered at (190, 190) and studying the integral as a function of the box size shows that

93

94

95

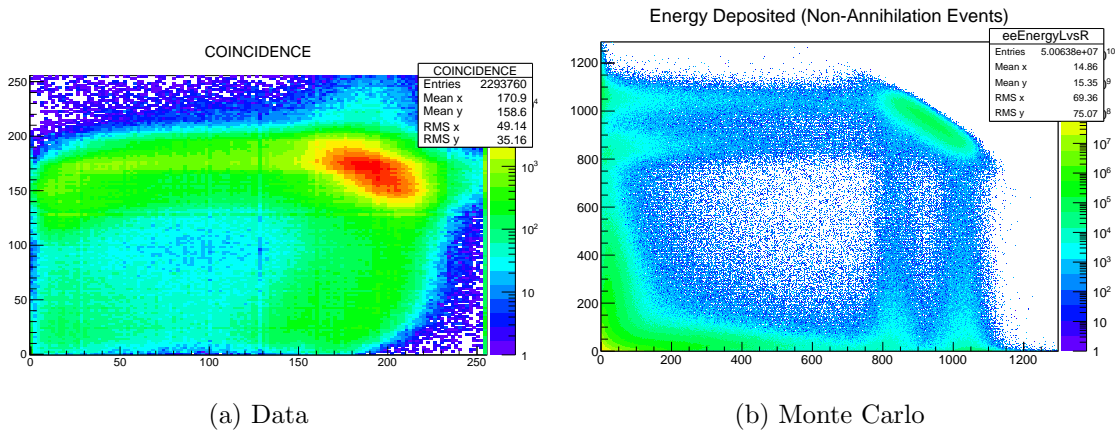


Figure 2: Symmetric Møller/Bhabha coincidences plots with a logarithmic scale for both data and Monte Carlo simulation.

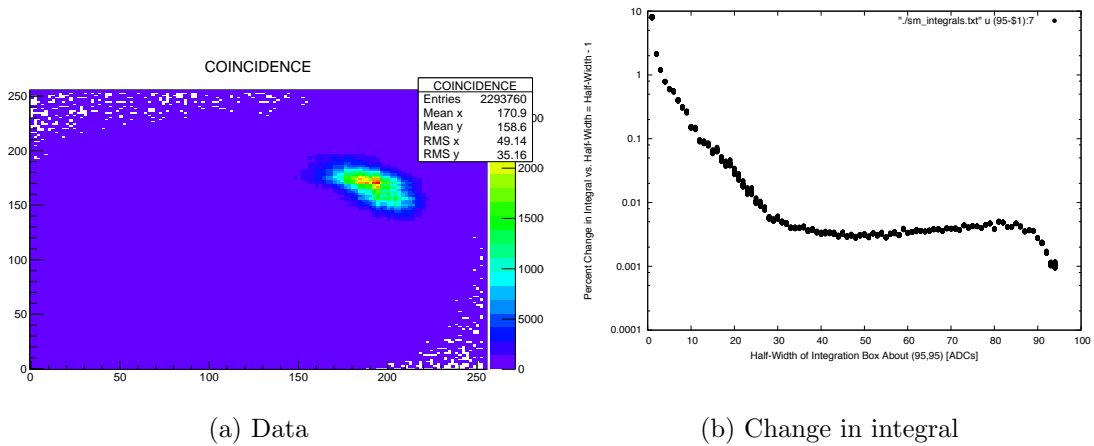


Figure 3: Symmetric Møller/Bhabha coincidence plot with a linear scale (left). On the right is the change in the integral over a square area centered at (190, 190) as a function of the box size..

96 the changes to the integral are less significant as the box size grows and are
 97 minimized for a box size around 80×80 .

98 - A separate fit to the measured magnetic field data in the volume important
 99 to the SYMB was made by B. Henderson and A. Schmidt to yield the fits
 100 needed for tracking SYMB events in the Monte Carlo. The resulting small
 field ($< \pm 30$ G) are shown in Fig. 4.

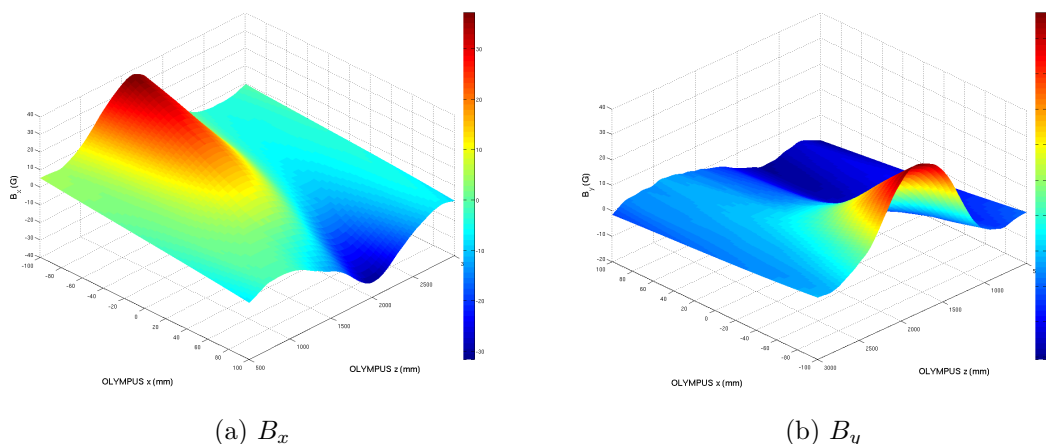


Figure 4: Optimized fits to the magnetic field in the volume relevant for the symmetric Møller/Bhabha detectors.

101

102 3.2 Beam Position Monitors

103 - U. Schneekloth organized and analyzed the calibration of the beam position
 104 monitors, BPMs.

105 - Knowledge of the beam position during data taking is crucial in analyzing the
 106 SYMB luminosity because the small angle, 1.29° , for symmetric scattering is
 107 very sensitive to the beam position and slope.

108 - The BPMs upstream and downstream of the target were readout by two sys-
 109 tems: Neumann and Libera. Only the first was readout by the OLYMPUS
 110 slow control during the February, 2012 running period. And unfortunately
 111 only the Libera system was available in 2013–2014 when the offline calibration
 112 was performed.

- 113 - To determine the relationship between the Neumann and Libera measures of
114 the beam position the time database of DORIS machine parameters was anal-
115 ysed.
- 116 - Then an absolute calibration was performed offline using a test stand with
117 a current flowing in a wire positioned inside the BPMs. The wire position
118 was surveyed and adjusted by micrometer screws while the Libera readout was
119 recorded.
- 120 - Thus the beam position and slope can now be determined for the OLYMPUS
121 data periods.
- The results of the calibration and comparison are summarized in Table 1

Table 1: Ratio of Neumann corrected to Libera values.

			$Ratio_x$	σ_x	$Ratio_y$	σ_y
positrons	Downstream	SL0-BPM1	1.000	0.009	1.015	0.040
	Upstream	SL2-BPM2	1.000	0.012	1.001	0.027
electrons	Downstream	SL0-BPM1	0.997	0.010	1.000	0.017
	Upstream	SL2-BPM2	0.999	0.013	0.999	0.022

122

123 3.3 12° GEM and MWPC Detectors

- 124 - On closer inspection of the GEM efficiency B. Henderson discovered and Ö. Ates
125 confirmed that several APV problems existed resulting in a noticeable pattern
126 of inefficiency which was averaged over by the clustering algorithms and large
127 bin size used previously.
- 128 - The resulting GEM efficiency varies from 90–95 %. Some improvement can be
129 made by averaging neighboring channels and new clustering algorithms. Ulti-
130 mate GEM efficiency should be better than 95 %. The remaining inefficiency
131 must be now incorporated into the MC simulation for the GEMs.
- 132 - The MWPC efficiency remains very high. With just a few dead wires the
133 MWPC overall efficiency is 97–99 % and even the area near the dead wires can
134 be recovered by requiring just two of the three XUV planes.

- 135 - Even with the reduced efficiency of the GEM detectors tracking through the
 136 12° telescopes should still be very efficient by allowing 4, 5, or 6-fold coinci-
 137 dences. Measurements using just the GEM or MWPC telescopes will provide
 138 an additional monitor of the luminosity and help to understand systematics.
- 139 - The alignment of the 12° tracking elements is highly accurate. Track residuals
 140 with all 6 elements fitted are of order $20 \mu\text{m}$, and around $300 \mu\text{m}$ with the tested
 141 GEM element taken out of the fit, implying a GEM resolution of $\sim 75 \mu\text{m}$ (see
 Fig. 5).

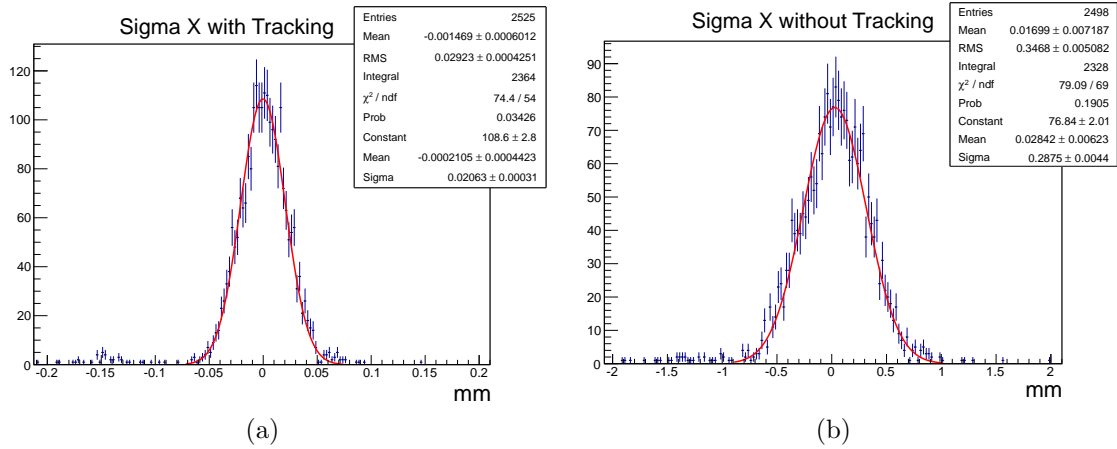


Figure 5: Residual of the 12-deg tracks in the left sector. Left (a): Track residual at left downstream element. Right (b): Track residual without including the testing element in the track fit. The resolution of the tested element is $\sim 75 \mu\text{m}$.

- 142
- 143 - Fig. 6 shows the momentum distribution of scattered leptons. The elastic scatter-
 144 ing events have been selected in coincidence with recoil protons for positrons
 145 and electrons with both polarities of the toroid magnetic field. The MWPCs are
 146 essentially less sensitive than WC to the low momentum electron background
 147 which allows for using the data collected at negative field polarity. Also shown
 148 is the coplanarity of lepton and proton tracks.

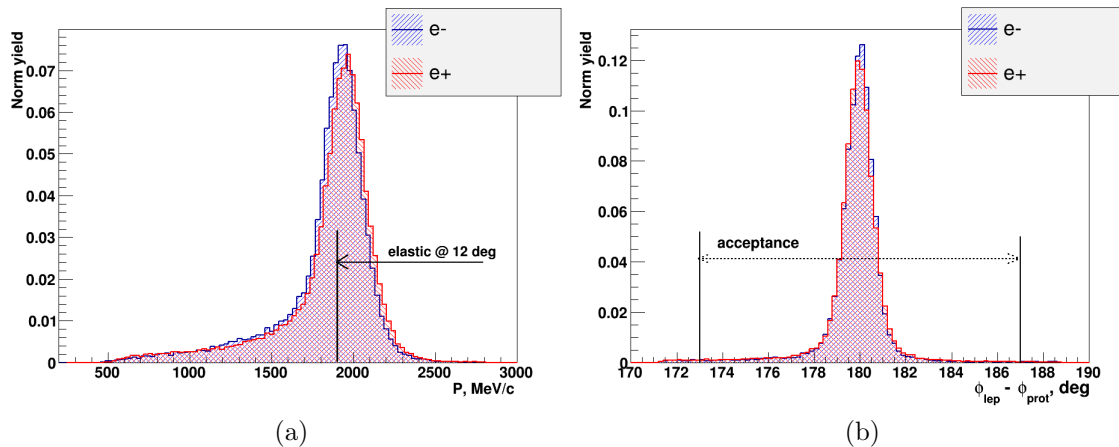


Figure 6: Left: Momentum distributions of elastically scattered electrons and positrons detected by 12° monitor in coincidence with recoil protons. Lepton tracks are reconstructed with the GEMs and MWPCs. Right: Lepton-proton coplanarity. Lepton and proton tracks are reconstructed using Kalman filter.

4 Time of Flight Detectors

149

- 150 - With tracking extended (see below) to the TOF detectors it is possible to
- 151 continue and improve the calibration.
- 152 - L.D. Ice and others have analyzed the TOF data using the track data. Fig. 7
- 153 shows the difference between the TOF bar number predicted by the tracking
- 154 and that actually hit (typically < 1).
- 155 - Similarly there is a strong correlation between the vertical position from track-
- 156 ing and that reconstructed from the time difference between the top and bottom
- 157 PMTs (see Fig. 8).
- 158 - The resolution around 100 mm is consistent with that achieved at BLAST.
- 159 - Fig. 9 shows the momentum versus time of flight for leptons and protons.
- 160 At higher momenta the separation is not so clear. L.D. Ice, R. Russell, and
- 161 J. Bernauer are investigating improving this by correcting the time of flight by
- 162 the actual path length.
- 163 - Electrons and protons are of course separated by their charge and opposite
- 164 curvatures in the magnetic field. But distinguishing positrons and protons

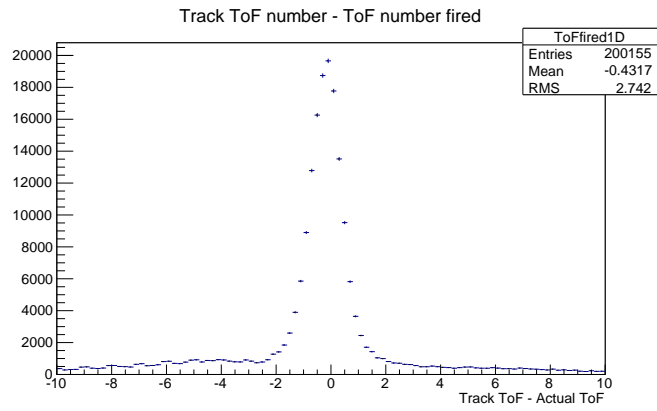


Figure 7: Difference between TOF bar number expected from tracking and as found in data.

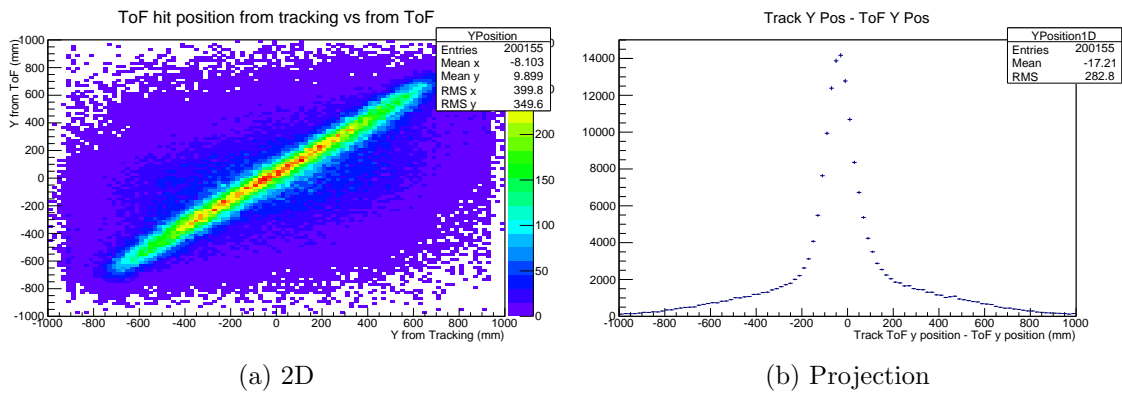


Figure 8: Comparison of vertical position in TOF from data and expected from tracking.

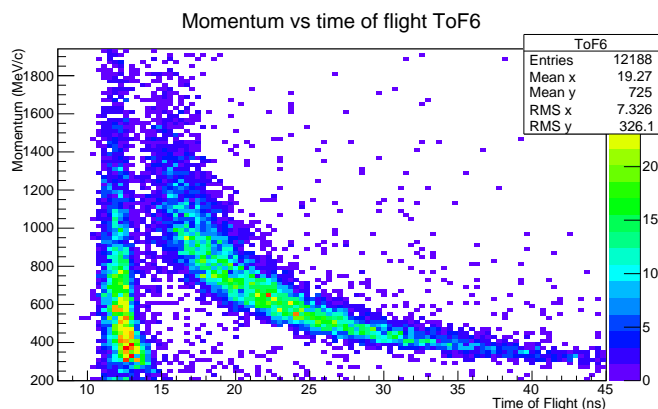


Figure 9: Momentum versus time of flight for ToF bar 6 showing the separation between leptons and protons.

165 will require a probabilistic approach based on these momentum versus time
 166 figures as well as other measures.

167 - R. Russell has investigated the energy deposited in the TOF as a function of
 168 the time of flight. The expected “sail” figure for protons is clear in Fig. 10.
 This can then be used to calibrate and monitor TOF gain. The same effect is

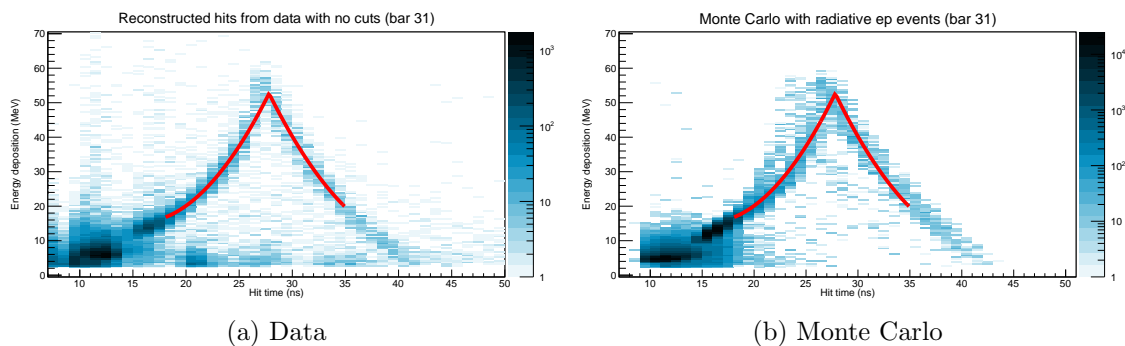


Figure 10: Energy deposited in TOF bar 31 as a function of the hit time from data and in Monte Carlo simulation. The “sail” shape corresponds to protons passing through the scintillator for higher energy protons, rising up to the peak and then falling as low energy protons are stopped in the scintillator.

169 nicely reproduced in the Monte Carlo (same figure) lending confidence to the
 170 TOF simulation.
 171

172 5 Track Reconstruction

- 173 - The main track reconstruction remains the elastic arm algorithm, EAA, imple-
174 mented by J. Bernauer. The EAA finds and fits tracks to the data accounting
175 for energy loss and multiple scattering. A separate program then extracts a
176 time to distance relationship (splines) from the fitted track. Possibly the splines
177 can be replaced by the algorithm described in the next section.
- 178 - The yields for electron and positron elastic scattering were shown at the PRC
179 meeting in October, 2013. They showed qualitatively that the track recon-
180 struction is working over the range of Q^2 accessible at OLYMPUS with good
181 agreement between electrons and positrons.
- 182 - As previously mentioned the tracking has been extended to the time of flight
183 detector (see above).
- 184 - Tracked data has also been released to the collaboration so everyone can start
185 developing their own analyses. Some of these will be shown in the next section.
- 186 - Future releases of tracked data will have some tracks deliberately removed to
187 “blind” the analysis and thus stop people selecting cuts that tune the result.
188 Also it will prevent premature release of results.

189 5.1 Alternative, Traditional Track Reconstruction

- 190 - Track reconstruction in the OLYMPUS wire chambers is not trivial. The inho-
191 mogeneous magnetic field means every drift cell has a different time to distance
192 relationship. Furthermore this relationship varies to the left and right of each
193 sense wire and each sense wire in a cell is different.
- 194 - Using MagBoltz it is possible to calculate gas properties. These can then be
195 used in a field mapping program like Garfield to determine lines of electron
196 drift and isochrones (see Fig. 11).
- 197 - The tangent point to each isochrone, extrapolated to the point where it crosses
198 the sense wire plane gives the distance from the sense wire for that track angle,
199 drift time, sense wire, magnetic field, and side (left or right) of the sense wire.
- 200 - The position where the track crosses the sense wire plane is needed to recon-
201 struct the track. But the range of distance versus time is large (see Fig. 12).

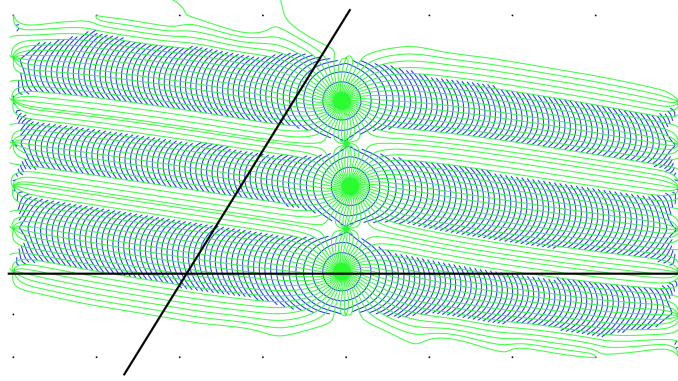


Figure 11: Fieldmap for a single drift cell showing lines of electron drift (green) and isochrones (blue). The desired reconstructed position for a track (angled line) is the point where the track crosses the sense wire plane (horizontal line).

202

203 - For a well defined condition: fixed track angle, fixed field, fixed sense wire,
 204 fixed side of the sense wire; the time to distance relationship is fairly simple
 205 (see Fig. 13). A cubic polynomial near the wire with a linear polynomial in the
 206 main drift region would be sufficient.

207 - D. Hasell has derived a fairly simple parameterization which gives the coeffi-
 208 cients for the polynomials as a function of the field, track angle, wire number,
 209 and side. The residual between this parameterization and the data from the
 210 field map is shown in Fig. 14. The deviation is mostly $< \pm 0.5$ mm which is
 211 comparable to the 1 mm stagger in the sense wires in a cell. However, this is
 212 based on assuming we know the gas mixture, that MagBoltz correctly calcu-
 213 lates the gas properties, and that the field mapping program correctly models
 214 the drift cells.

215 - It is likely that this approach will just provide a starting point for track recon-
 216 struction and that the parameterization will have to be optimized by iterating
 217 over the found tracks.

218 - Nevertheless this work has begun and the preliminary result for finding track
 219 “stubs” in a super-layer of the wire chamber is shown in Fig. 15. The main peak
 220 indicates a resolution around $400 \mu\text{m}$ which is consistent with what was ob-
 221 tained at BLAST. However, there are also mis-identified “stubs” and a sizable
 222 background.

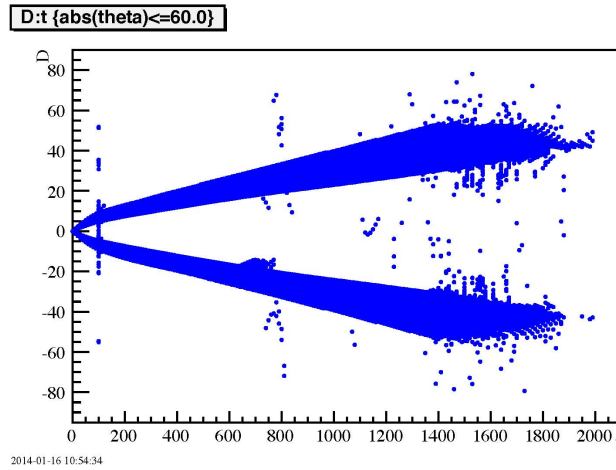


Figure 12: Drift distance versus drift time for all sense wires in a cell, all possible magnetic fields, the possible range of track angles, and for left (positive) and right (negative) sides of the wire.

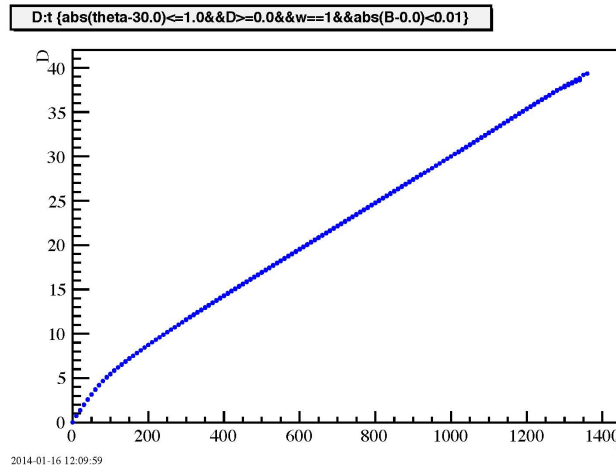


Figure 13: Distance versus drift time for a well defined condition.

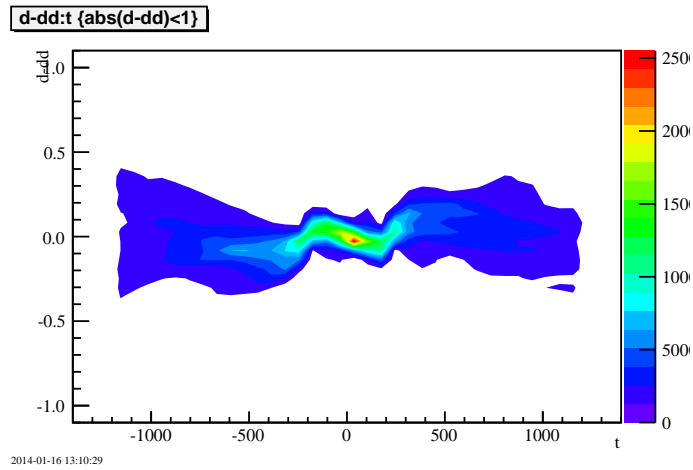


Figure 14: Difference between parameterization of time to distance relation and the input data generated by the field map program and gas properties.

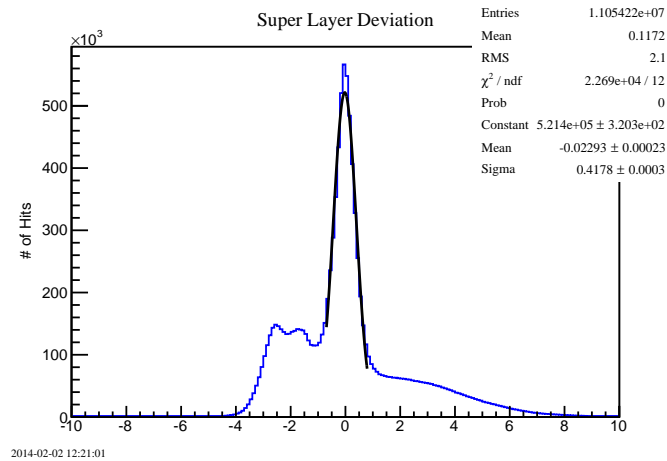


Figure 15: Residual from fitting a straight line to a track “stub” in a super-layer of the OLYMPUS wire chambers.

- 223 - Work will continue to improve this and to connect the “stubs” to form tracks.
- 224 - Even if this work doesn’t result in a reasonable production-quality track re-
- 225 reconstruction algorithm it can help understand the process and possibly supply
- 226 track candidates for the elastic arm algorithm. The parameterization could
- 227 also be applied inside the elastic arm algorithm and/or in digitizing the wire
- 228 chamber hits in the Monte Carlo.

229 6 Analysis

230 The current selection of tracked runs have been distributed to the collaboration so
 231 everyone can participate in the analysis. Some of the results from the various groups
 232 are given here.

- 233 - The momentum resolution, $\Delta P/P = 0.12$, calculated by J. Bernauer is shown
 in Fig. 16.

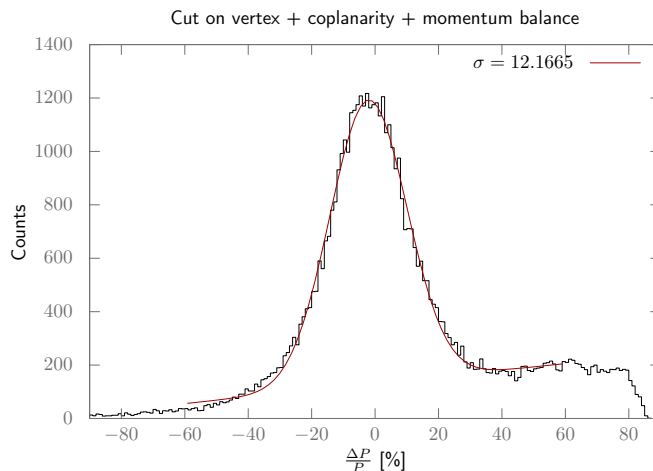


Figure 16: Track momentum resolution.

- 234
- 235 - The PNPI group has compared the electron and positron elastic scattering yield
- 236 with expected yields from Monte Carlo. These are shown in Fig. 17. Arbitrary
- 237 normalizations have been applied to both distributions and qualitatively the
- 238 agreement is encouraging.

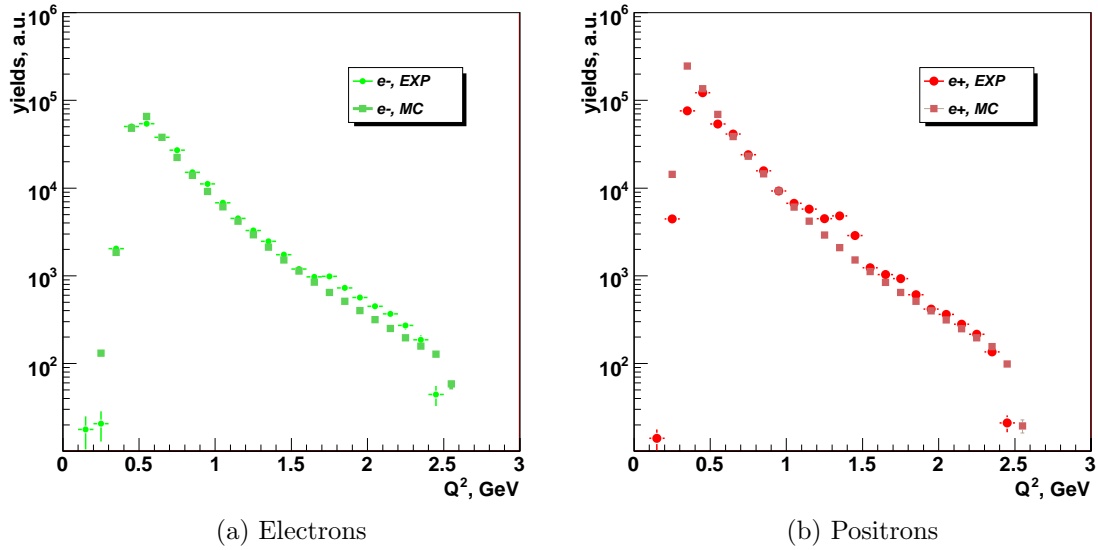


Figure 17: Comparison of yield from tracked data and Monte Carlo simulation for electron (left) and positron (right) beams with arbitrary normalizations for both.

- 239 - N. D’Ascenzo’s analysis clearly shows the elastic scattering event resolved from
- 240 background in Fig. 18 with simple cuts and can reconstruct the beam energy
- 241 with a resolutions around 53 MeV (see Fig. 19).

- 242 - The AANL (Yerevan) group has also analysed the tracked data. The reduced
- 243 “ χ^2 ” for a sequence of event selection criteria is shown in Fig. 20. The recon-
- 244 structed beam energy and x and y components of the track momenta are given
- 245 in Fig. 21.

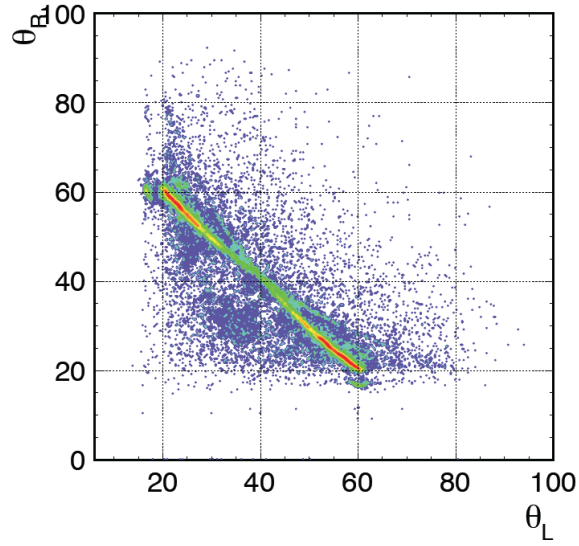


Figure 18: Angular correlation between scattering angle measured in the left sector versus the angle in the right sector. Event selection required reconstructed beam energy to be within 200 MeV and tracks to be coplanar within 4° .

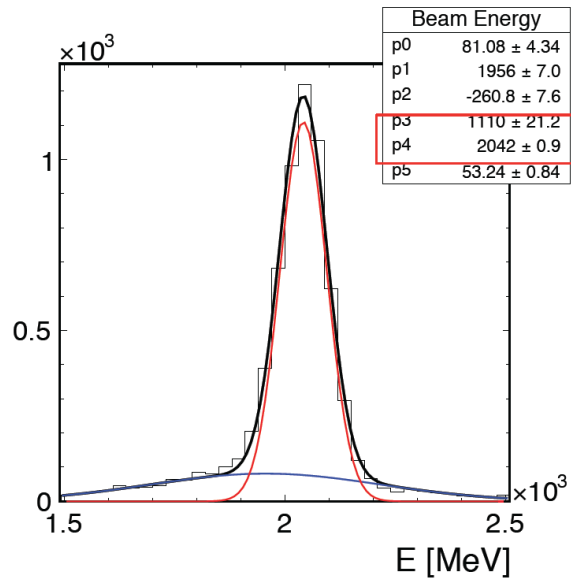


Figure 19: Beam energy reconstructed from lepton and proton scattering angles for lepton scattering angles in the range 32° – 40° .

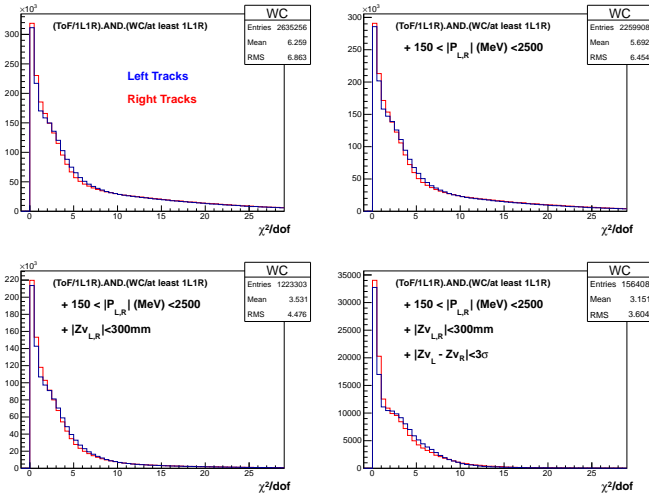


Figure 20: Reduced “ χ^2 ” for reconstructed tracks with electron tracks in the left (blue) and right (red) sectors. The different plots correspond to progressive cuts on the event selection (UL - tracks both left and right, UR - cuts on track momenta, LL - tracks from target,, and LR - vertex cut).

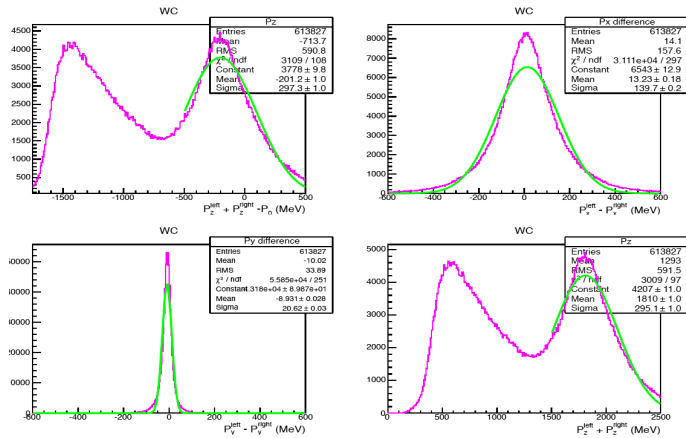


Figure 21: Reconstructed beam energy and reconstructed x , and y components of momentum.

246 6.1 Radiative Corrections

- 247 - R. Russell and A. Schmidt have written a radiative event generator based on
248 the Mainz generator (J. Bernauer) and incorporated it into the OLYMPUS
249 Monte Carlo framework.
- 250 - The radiative corrections include: soft two photon exchange, vertex corrections
251 including self-energy, initial and final state bremsstrahlung for both lepton and
252 proton, and vacuum polarization. It does not include hard two photon effects.
- 253 - The radiative corrections agree with Maximon and Tjon in the low energy limit.
- 254 - The radiative corrections are intended to be part of a common software package
255 for all the two-photon experiments (Jlab, Novosibirsk, and OLYMPUS) to
256 simplify comparing results.
- 257 - The MIT code has been tested and compared with the Novosibirsk code and
258 found to agree. Fig. 22 shows the invariant matrix element as a function of the
259 lepton polar angle and lepton momentum for photon scattering angles $\theta = 10^\circ$
260 and $\phi = 120^\circ$ and lepton azimuthal angle $\phi = 0^\circ$ for both MIT and Novosibirsk
261 codes and the difference between the two ($< 0.01\%$).

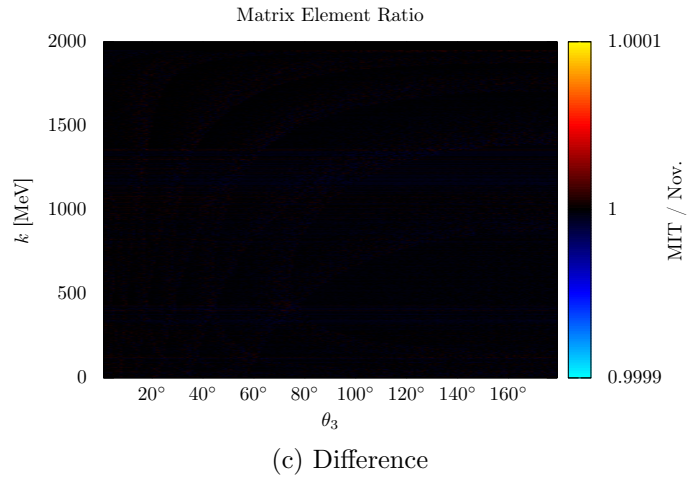
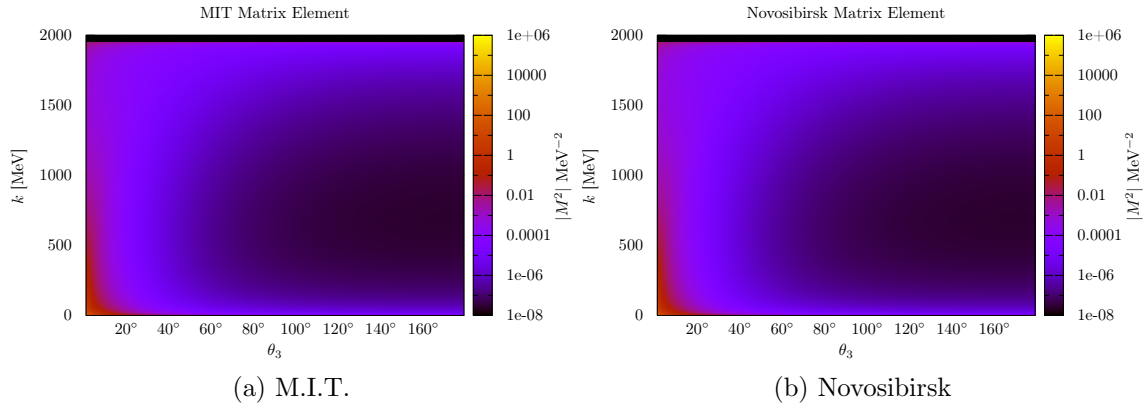


Figure 22: Comparison of radiative corrections calculated using the MIT and Novosibirsk generators.

262 **7 Miscellaneous**

- 263 - The NIMA paper describing the experimental hardware, electronics, and oper-
264 ation was accepted for publication - R. Milner, et al. The OLYMPUS Experi-
265 ment, NIMA (2013), 10.1016/j.nima.2013.12.035.
- 266 - A paper describing the OLYMPUS target and vacuum system is nearly ready
267 for submission to NIM.
- 268 - A. Schmidt (radiative corrections) will give a talk at APS, Savannah, March
269 3–7, 2014.
- 270 - The next OLYMPUS collaboration meeting will be held at Mainz, March 10–
271 12, 2014 and include a one day workshop specifically to address issues with the
272 luminosity monitors.
- 273 - J. Diefenbach will give a talk on OLYMPUS at the DPG meeting in Frankfurt,
274 March 17–21, 2014.
- 275 - R. Perez Benito (SYMB) and R. Russell (radiative corrections) will also give
276 talks at DPG.
- 277 - An OLYMPUS session with four presentations has been held at the APS/DNP
278 fall meeting 2013 in Newport News, October 23–26, 2013.
- 279 - M. Kohl has given invited talks on two-photon exchange including OLYMPUS
280 at the APS/DNP fall meeting 2013 in Newport News, October 23–26, 2013, at
281 the EINN2013 workshop in Pafos, Cyprus, October 28–November 2, 2013, and
282 at the PRISMA seminar at Mainz University on November 27, 2013.

283 **8 Summary**

284 The analysis of the OLYMPUS data collected in 2012 is difficult and complex but
285 steady progress is being made. More people are active in the analysis. The results
286 obtained to date are encouraging and hopefully indicate that good, final results will
287 be obtained.

288 If there are questions about anything in this report perhaps it is easier and more
289 efficient to arrange a phone or video conference.